



Original article

Synthesis, characterization and evaluation of deacetylated xanthan derivatives as new excipients in the formulation of chitosan-based polyelectrolytes for the sustained release of tramadol

Meriem Boudoukhani ^{a,*}, Madiha M. Yahoum ^a, Sonia Lefnaoui ^b, Nadji Moulai-Mostefa ^a, Manuel Banhobre ^c

^a LME, Faculty of Technology, University of Medea, Ain D'Heb, Medea, Algeria

^b Faculty of Sciences, University of Medea, Ain D'Heb, Medea, Algeria

^c INL, International Iberian Nanotechnology Laboratory, Braga, Portugal

ARTICLE INFO

Article history:

Received 12 June 2019

Accepted 23 September 2019

Available online 25 September 2019

Keywords:

Xanthan gum

Desacetylation

Chitosan

Matrix tablets

Sustained release

Tramadol

ABSTRACT

This paper addressed the application of deacetylated xanthan (XGDS) and chitosan (CTS) as a mixture blend forming hydrophilic matrices for Tramadol (TD) sustained release tablets. XGDSs derivatives were obtained by alkaline treatment of xanthan gum (XG) with various degrees of deacetylation (DD). The obtained products were characterized in terms of structural, thermal and physicochemical properties. Different tablet formulations containing CTS/XGDSs were prepared by direct compression method and compared to CTS/XG tablets. Flow properties of powder mixtures and pharmaceutical characteristics were evaluated. The dissolution test of TD was realized under simulated gastric and intestinal conditions to achieve drug release more than 24 h. All developed tablets were found conforming to standard evaluation tests. It was shown that CTS/XGDSs matrices ensure a slower release of TD in comparison with CTS/XG based formulations. Meanwhile, increasing DD resulted in a decrease of drug release. In addition, TD release from XGDS matrices was faster at pH (6.8) than at acidic pH (1.2). The matrix tablets based on CTS/XGDS4 (DD = 98.08%) were selected as the best candidates compared to the other systems in prolonging drug release. The optimal formulation was found to release 99.99% of TD after 24 h following a non-Fickian type.

© 2019 The Authors. Production and hosting by Elsevier B.V. on behalf of King Saud University. This is an open access article under the CC BY-NC-ND license (<http://creativecommons.org/licenses/by-nc-nd/4.0/>).

1. Introduction

Despite recent developments in pharmaceutical formulation, the oral route remains the main way of administration because it presents the simplest route for drug absorption (Wise, 2000). Conventional oral dosage forms allow an immediate release of the drug (Ghori and Conway, 2015). Therefore, frequent administration is required for the active ingredient with a short biological half-life and the efficacy of the administered drug being limited to its residence time in the blood (Wen and Park, 2011). In order to overcome these disadvantages, the modified release dosage forms

have been developed and thus, sustained-release forms are the most studied (Yihong, 2009).

The sustained-release formulations are mainly hydrophilic matrices continuously releasing active ingredients for a prolonged period. For this purpose, the use of natural polymers in the formulation of hydrophilic matrix tablets is very frequent, and the most widely used polymers are polysaccharides, including polyelectrolyte molecules which are composed of negatively charged polysaccharides, such as carrageenan or xanthan gum (XG) and positively charged polysaccharides like chitosan (CTS) (Alvarez-Lorenzo et al., 2013).

Native polysaccharides as well as their functionalized derivatives are considered as very promising excipients for drug delivery. This increased interest for their use is due to their particular properties, mainly their abundance, biocompatibility, and reduced costs.

It was shown that XG is an excellent excipient for the sustained release of drugs. The main property of this polysaccharide is to have significant thickening power, even at low concentrations and a strong shear-thinning character (Roy et al., 2014). Thus, XG

* Corresponding author.

E-mail address: boudoukhani.meriemlme@gmail.com (M. Boudoukhani).

Peer review under responsibility of King Saud University.



Production and hosting by Elsevier

is used in aqueous systems as viscosifying and/or stabilizing agent in dispersions like emulsions and suspensions (García-Ochoa et al., 2000). In addition, XG has a water-absorbing capacity, which prevents the fast release of the incorporated drug by its entrapment within a thick gelled layer. When used alone or in combination with other macromolecules (cellulose derivatives, polyvinylpyrrolidone, karaya and guar gum), XG-based matrices demonstrated a great ability to generate a drug release profile close to zero (Mughal et al., 2011). Xanthan gum was also evaluated as a hydrophilic matrix for controlled-release preparations because it not only delays the release of drugs, but also provides time-independent release kinetics with advantages of biocompatibility and inertia (Ramamany et al., 2011).

One of the positively charged natural polymers that have been widely studied as a potential drug vehicle is CTS (Elsayed et al., 2009; Rekha and Sharma, 2009; Ramasamy et al., 2013). It has been mixed with various polymers to modify the release of active ingredients and protect therapeutic biomolecules (Chen et al., 2013; Bhattarai et al., 2010). Among the natural polymers associated with CTS, carrageenan, pectin, alginate and XG are the most employed (Martínez-Ruvalcaba et al., 2007; Volod'ko et al., 2014). Moreover, the use of CTS and XG in the form of polyelectrolyte complex (PEC) as an excipient mixture in the formulation of delayed dosage forms has been widely reported. Indeed, the PECs based on CTS/XG blends were likely used as gastrointestinal hydrogels drug delivery systems (Dumitriu and Chornet, 1997), or as films for wound healing (Bellini et al., 2015) as well as in tissue engineering (Veiga and Moraes, 2012), in capsules formulations (Popa et al., 2010), in encapsulation systems as Beads (Fareez et al., 2015), in microspheres (Umadevi et al., 2010), and in direct compression tablets (Corti et al., 2008).

The formation of the PECs is due to the ionic attractive forces between CTS positively charged amino groups and negatively charged carboxylic groups in XG (Martínez-Ruvalcaba et al., 2007). Therefore, the characteristics of the produced PECs are largely dependent on the physicochemical properties of the used polymers. Previous studies have mostly focused on the pyruvic acid content and the molecular weight of XG as the most crucial factors (Qinna et al., 2015; Luo and Wang, 2014), but to our knowledge there is no studies reported on the properties of PEC formed by the desacetylated xanthan (XGDS) and CTS.

Extensive research has shown that XG has been modified by varying the levels of acetyl and/or pyruvyl groups (Roy et al., 2014), or chemical modification by grafting new entities on the hydroxyl functions (Ghorai et al., 2013; Kumar et al., 2012), or on carboxylic acid functions of the XG macromolecule (Mendes et al., 2013). By eliminating the acetyl group from XG, deacetylation reaction allows the increase of the negative charge of the macromolecule and thus offers more opportunity when used in combination with other biopolymers. The utility of the deacetylation reaction of xanthan was found to have an impact on the various properties of the deacetylated derivatives (Callet et al., 1987; Tako and Nakamura, 1984; Khouryieh et al., 2007). In addition, the decrease of the molecular weight and the improvement of the solubility of XGDS are considerable advantages when used as pharmaceutical excipients.

Up to now, far too little attention has been paid to XGDS, despite the fact that the desacetylation reaction in alkaline medium is very attractive because it requires few chemicals and simple treatment to lead to new features of the polysaccharide. Furthermore, no previous studies have investigated the CTS/XGDS mixture as a pharmaceutical excipient in sustained drug release.

Our proposal is to achieve new pharmaceutical excipients based on PECs formed by CTS/XGDSs. This is dependent on the fact that the hydroxyl and carboxylic groups in XGDS are strongly acidic, which allows for polymer ionization and interaction with the

cationic CTS. The CTS/XGDSs mixture was utilized to form hydrophilic matrices in order to sustain the release of Tramadol (TD) used as drug model. The ability of CTS/XGDS mixture to modulate the release of TD will strongly depend on the properties of the formed PEC and therefore the degree of deacetylation (DD) of each derivative of XGDS.

TD is an analgesic agent, frequently used in the treatment of a variety of pain syndromes (Beakley et al., 2015). It is a 4-phenylpiperidine analog to codeine, but it has less potential for abuse and respiratory depression. When administered orally, TD has rapid absorption and distribution. Indeed, the maximum serum concentration being reached after 2 h, TD undergoes a first pass metabolism and has a half-life of 5–6 h (Vazzana et al., 2015). Due to its hepatic metabolism and renal clearance, development of oral extended-release forms is required to reduce the daily intake of patients and to maintain an effective drug plasma concentration. Formulations of controlled release dosage forms of TD were reported by several authors (Mishra et al., 2006; Pergolizzi et al., 2011; Mabrouk et al., 2018).

The present study focuses on the development of TD extended release matrix systems using a polyelectrolytic complexation mechanism between CTS and XGDS. Hydrophilic matrices prepared by combining these two oppositely charged biopolymers were investigated for the first time.

Based on the above considerations, the aim of this work was first to prepare XGDS derivatives in an alkaline environment with different DD. The physicochemical, thermal and rheological properties of XGDSs were examined by FTIR, TGA, DSC, and HPLC analysis. After that, physical blends of CTS/XGDS were used to formulate hydrophilic matrix tablets by direct compression method. The release kinetics from the TD loaded dosage forms was studied *in-vitro* and the obtained dissolution data were fitted to adequate mathematical models in order to predict the influence of the used PECs on the mechanism of drug release.

2. Material and methods

2.1. Materials

Xanthan gum (XG) with a molecular weight (Mw) of 2.5×10^6 g/mol and 38% of acetylated group was purchased from Solvay (France). Chitosan (CTS) with Mw of $190,000 \text{ g mol}^{-1}$ and 81.4% deacetylated was purchased from Sigma Aldrich (Iceland). Tramadol hydrochloride (TD), lactose monohydrate (LM) and magnesium stearate (STMg) were kindly provided by Soidal (Medea, Algeria). The other analytical reagents (sodium hydroxide, hydrochloric acid, potassium hydroxide, phosphoric acid, sulfuric acid and ethanolic alcohol) were supplied by Merck (Switzerland).

2.2. Deacetylation of native xanthan

The methodology used in this study is based essentially on the works of Tako and Nakamura (1984) with some modifications. The deacetylation reaction consisted of an alkaline hydrolyze of XG (Fig. 1) using sodium hydroxide aqueous solutions at different concentrations (0.0025, 0.005, 0.0075 and 0.01 mol/L). The deacetylation was performed on XG aqueous solutions (1%, in wt.) where, erlenmeyer flasks filled with 125 mL of each solution were placed on a magnetic agitator at 300 rpm. All reactions were carried out at a temperature of 25 °C during 3 h. The obtained products were then neutralized with a hydrochloric acid solution (2 M). The modified polysaccharides were recovered by precipitation with ethanol 96° in the proportion of 1:4 (v/v), dried at 56 °C until a constant weight was achieved and then pulverised to have a fine particle size. According to the US procedure (USP 39, 2016) for sieving

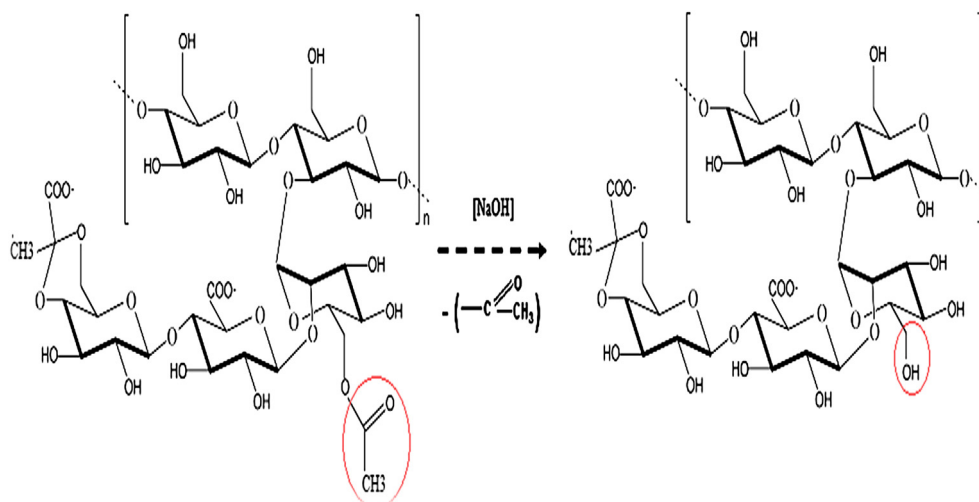


Fig. 1. Scheme of deacetylation reaction of xanthan gum.

analysis, a mass of XGDS sample was placed on the stack of sieve (200, 150 and 50 μm) in mechanical shaker. The nest of sieves was completed by a well-fitting pan at the base and a lid at the top. The sieving analysis is considered as complete when the weight of any of the test sieves does not change by more than 5% of the previous weight on that sieve. The mass fraction on the 150 μm sieve was used in the characterization and formulation tests.

2.3. Characterization of deacetylated xanthan derivatives

2.3.1. Determination of the degree of deacetylation

Acetyl levels of native xanthan (XG) and deacetylated xanthan (XGDS) were determined using a titration method. Briefly, 0.095 g of polymer sample (XG or XGDS) was dissolved in 7.5 mL of distilled water. After stirring for 30 min, 1.5 mL of NaOH (1 M) was added and the vial was closed and agitated during 2 h. The sample was titrated with H_2SO_4 (1 M) using phenolphthalein as colored indicator. The acetyl group (A_c) was calculated using Eq. (1):

$$A_c = \frac{[6.005 * (B - A) * F]}{W} \quad (1)$$

where B is the required volume of H_2SO_4 for the blank, A is the required volume of H_2SO_4 for the sample, F is the concentration factor of H_2SO_4 and W is the mass of the sample.

The degree of deacetylation (DD) was deduced using Eq. (2):

$$DD(\%) = (100 - A_c) \quad (2)$$

2.3.2. Determination of the degree of solubility

The degree of solubility (S) was determined by the method reported previously by Du et al. (2012) and Li et al. (2014). Briefly, a certain amount of powder sample (0.10 g) was dispersed with 24.90 g of ice and put at a temperature of (0 ± 0.5 $^\circ\text{C}$) in an ice bath with low speed stirring until the total melting of ice. Afterwards, this mixture was submitted to centrifugation during 20 min at 4500 rpm; subsequently a weight of 10 g of supernatant was dried to a constant weight at 105 $^\circ\text{C}$. The solubility degree was calculated using Eq. (3):

$$S(\%) = \frac{m * 2.5}{w} * 100\% \quad (3)$$

where m is the dry matter content and w is the total mass of the sample.

2.3.3. Determination of the average molecular weight

The protocol used to determine the molecular mass was similar to that followed by Masuelli (2014). Briefly, a stock solution was first prepared where a quantity of 0.27 g of XG and XGDSs were dissolved in 200 mL of a saline solution (NaCl, 0.01 M). An Ubbelohd capillary viscometer was utilized at room temperature (25 ± 0.1 $^\circ\text{C}$).

Molecular weights were calculated using the Mark-Howink relationship (Eq. (4)) of intrinsic viscosity to the molar mass of the biopolymer.

$$[\eta] = K * M^a \quad (4)$$

where K and a are the characteristic constants of the polymer-solvent pair at a given temperature, and their values are generally limited with $K = 2.79 * 10^3 \text{ cm}^3/\text{g}$ and $a = 1.2754$ at 25 $^\circ\text{C}$ (Tinland and Rinaudo, 1989; Yahoum et al., 2016).

2.3.4. Fourier transform infra red spectroscopy

Fourier Transform Infrared (FT-IR) spectra of XG and XGDS (with different DD) were determined using a FT-IR spectrophotometer (Bruker, Germany) with a resolution of 4 cm^{-1} . It was used for a range of electromagnetic spectra varying between 400 and 4000 cm^{-1} in order to observe the functional groups.

2.3.5. Thermal analysis

Calorimetric (DSC), thermogravimetric (TGA), and differential thermal (DTA) analyses were performed using equipment TGA/DSC 1 STARE System. The thermal analysis was carried out by subjecting the material to a controlled temperature program with a linear variation of temperature (dynamic conditions). The experimental parameters used in these analysis were: average weight of samples between 0 and 5000 mg, heating rate of 5 $^\circ\text{C min}^{-1}$ (25–120 $^\circ\text{C}$) and 10 $^\circ\text{C min}^{-1}$ (120–900 $^\circ\text{C}$), temperature range varying between 25 and 900 $^\circ\text{C}$, argon atmosphere (inert atmosphere) and a flow rate of 30 mL/min. The pans were closed.

2.3.6. Scanning electron microscopy

Surface characterization of different samples was realized by scanning electron microscopy (SEM); FEI Quanta FEG 650, connected with a microscope control supervisor V6.2.8 build 3161) at the required magnification and room temperature. A working distance of 10 μm was maintained, and an acceleration voltage of 10 kV was used. A drop of the native and modified xanthan

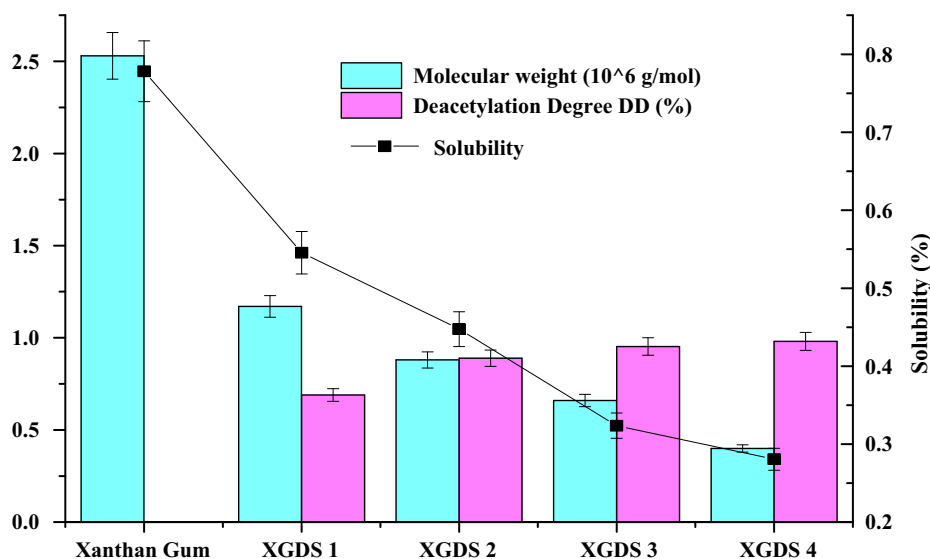


Fig. 2. Variations of molecular mass, deacetylation degree and solubility of native and deacetylated xanthan derivatives.

aqueous solution although the precise role of acetyl groups in promoting solubility is not indicated (Du et al., 2012). Similar results were found with Konjac glucomannan gum where it was found that the solubility decreased exponentially when the DD increased (Li et al., 2014).

3.1.2. Chemical structure

Infrared spectra of XG and XGDSs (Fig. 3) confirmed the deacetylation reaction of the native XG after basic treatment of each sample. A difference between FT-IR spectra for native and modified samples is observed by the decrease in peak transmittance at about 1724 cm^{-1} , which has been attributed to the acetyl group. It is clear that DD is proportional to the peak absorption intensity at 1724 cm^{-1} . The spectra showed that the acetyl group

was removed by modification in alkali conditions. Tako and Nakamura (1984) suggested that acetate residues contribute to the intermolecular association and that the side chains of XG may become more flexible after deacetylation. Absorption at 1724 cm^{-1} refers to the absorption of acetyl stretching vibrations $\text{C}=\text{O}$. On the other hand, the other characteristic peaks of XG and its derivatives are constant without any apparent modification which indicates the specificity of the deacetylation reaction. These results are similar to those obtained by several authors (Siddhartha and Biswanath, 2014; Yahoum et al., 2016) for native XG. While comparing FT-IR spectrum of XGDS1, XGDS2, XGDS3 and XGDS4, the characteristic peaks around 3300 , 2900 and $800\text{--}1100\text{ cm}^{-1}$ which are common to all polysaccharides, represent broad peaks of OH, CH and CH_2 bonds respectively. The maximum value

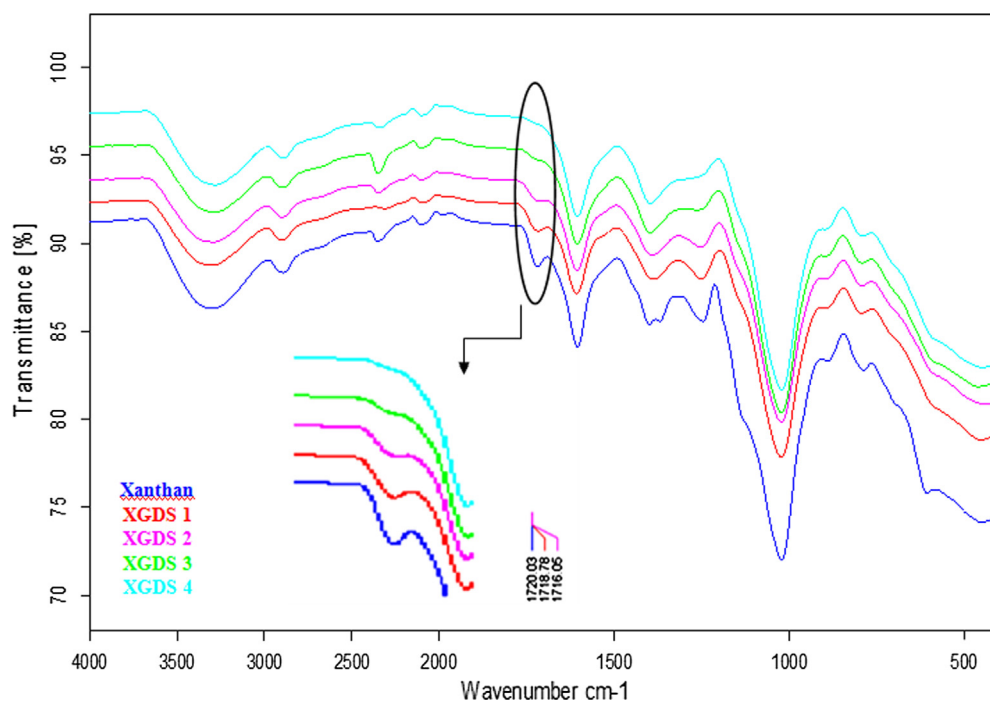


Fig. 3. FTIR spectra of native and deacetylated xanthan derivatives.

decreases gradually as the amount of NaOH increases, demonstrating the increase in the degree of modification. In particular, the peak disappears when the amount of alkaline pentasaccharide units reaches complete deacetylation for XG, which is in agreement with the literature (Du et al., 2012; Li et al., 2014; He et al., 2016).

3.1.3. Thermal properties

DSC is the most common technique for polymer characterization. It allows a quantitative analysis of the transitions in energetic terms if the polymer undergoes a change of physical state such as a fusion or transition from a crystalline form to another one. The enthalpic curves representing the evolution of the heat flux as a function of temperature (Fig. 4) show that a peak has been absorbed at 720 °C for pure XG, while other peaks are absorbed at 730, 653, 720 and 685 °C for XGDS1, XGDS2, XGDS3 and XGDS4, respectively. It was observed from the DSC profiles, that all samples were characterized by two thermal events. The first endothermic event, centered at about 100 °C is attributed to the loss of water associated with the hydrophilic groups of the polymers while, the second two exothermic peaks correspond to the thermal degradation of the polymers. The endothermic peak was attributed to the evaporation of water molecules residing in XG, which roughly reflects the water retention capacity. Moreover, XG showed a lower temperature of the endothermic peak compared with XGDSs, which suggests the decrease of the water retention capacity. In the thermograms of XG derivatives, two unequal exothermic peaks appeared between 300 and 800 °C, caused by the pyrolysis of XGDSs. In general, a lower crystallinity of the sample leads to a lower exothermic temperature.

Overall, the thermal characteristics of each sample were similar due to the alkaline deacetylation. The diminished acetyl group content of XG helped not only to reduce steric hindrance and reinforce the intermolecular interaction but also to increase the resistance to thermic degradation. Indeed, XGDS showed higher exothermic peaks of temperature than XG. However, the exothermic peak temperature of XGDSs did not increase steadily with increasing DD. These results are similar to those found for deacetylated Konjac glucomannan gum (Li et al., 2014).

TGA analysis was performed to study changes in the mass of samples with increasing temperature. Fig. 5 shows the percentage of decomposition of native and deacetylated xanthan. Analysis of thermograms shows that native XG had two-stage decomposition. The first stage was observed between 0 and 120 °C with a 100% weight loss that may be caused by the dehydration of all studied samples in addition to the loss of volatile molecules (He et al., 2016; Makhado et al., 2018). The second stage observed in the case of XG was obtained at high temperature (above 200 °C) and was

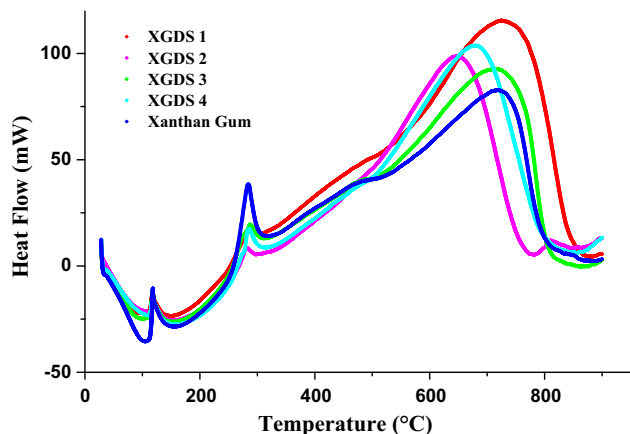


Fig. 4. DSC thermogram curves of native and deacetylated xanthan derivatives.

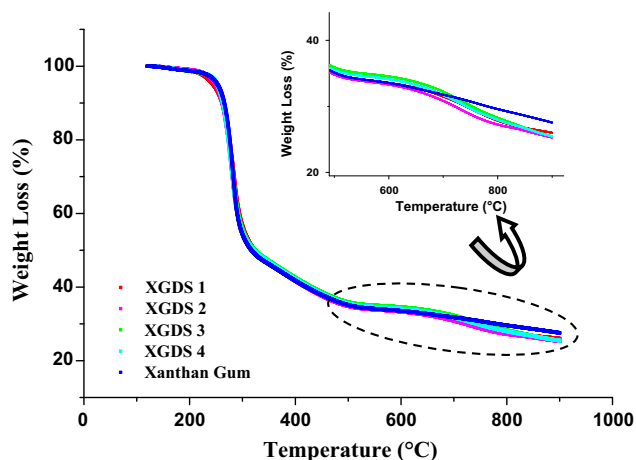


Fig. 5. TGA thermogram curves of native and deacetylated xanthan derivatives.

attributed to the degradation of the compounds due to deacetylation reactions with a mass loss of 33.33% at 540 °C; the weight reduction rate increased with an increase in temperature. The obtained temperatures in the second stage of decomposition were different in the case of XGDSs, where the weight losses are from 27.80% at 800 °C, 28.89% at 758 °C, 30.47% at 740 °C and 29.68% at 747 °C, for XGDS1, XGDS2, XGDS3 and XGDS4, respectively. These results showed that the variation in the second stage of TGA thermograms was due to the variation of polar groups in the structure of samples, in particular the hydroxyl groups (Li et al., 2016).

3.1.4. Morphological characterization

SEM was employed to show the morphological characteristics of the studied biopolymers (Fig. 6). The obtained images indicated significant changes of the surface morphology of XG after reacting. The SEM micrographs showed that XG particles (Fig. 6a) have an amorphous, porous nature and smooth surface, as reported by Makhado et al. (2018). Whereas those of XGDS have a smooth surface, with an elongated and thin shape, as illustrated in Fig. 6b–e. The morphology of XGDS samples appeared homogenous, indicating a uniform size distribution. Additionally, the micrographs showed intact granules allowing their use as pharmaceutical excipients.

3.2. Compatibility study of drug and polysaccharides

Similar to DSC (Fig. 7a), TGA analysis allows to study the thermal compatibility of an active pharmaceutical ingredient (API) with multiple excipients. TGA profiles were used to investigate the thermal stability of XG, XGDS, TD, CTS, and their physical mixture (Fig. 7b). All samples display two main weight loss regions. The first region ranged between 25 and 150 °C is attributed to the removal of physically adsorbed water. The second region represents the largest weight loss corresponding to the degradation of components at levels of 80.27, 79.74, 76.84, 99.73, and 60% corresponding to XG-TD, XGDS-TD, CTS-TD, TD and CTS, respectively. In addition, the DTA profiles of samples deduced from TGA data (Fig. 7c) exhibit the main decomposition peaks at 281, 277, 265 and 303 °C, for XG, XGDS, TD and CTS. Data for polysaccharides, including XG and CTS were reported by Zohuriaan and Shokrolahi (2004); they suggested that among these two biopolymers, CTS has the highest thermal stability. Otherwise, TGA analysis of TD in the presence of CTS, XG and XGDS showed that all materials underwent decomposition above the temperature of 250 °C which means that the presence of these excipients does

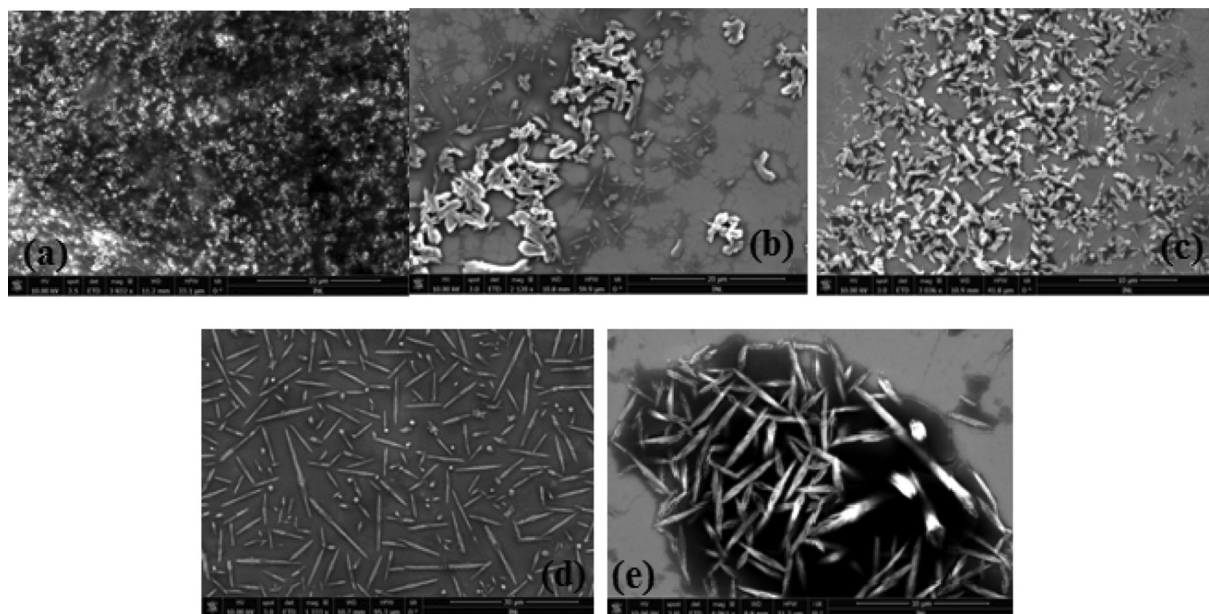


Fig. 6. SEM images at magnification ($\times 1000$) of (a) native xanthan, (b) XGDS1, (c) XGDS2, (d) XGDS3, (e) XGDS4.

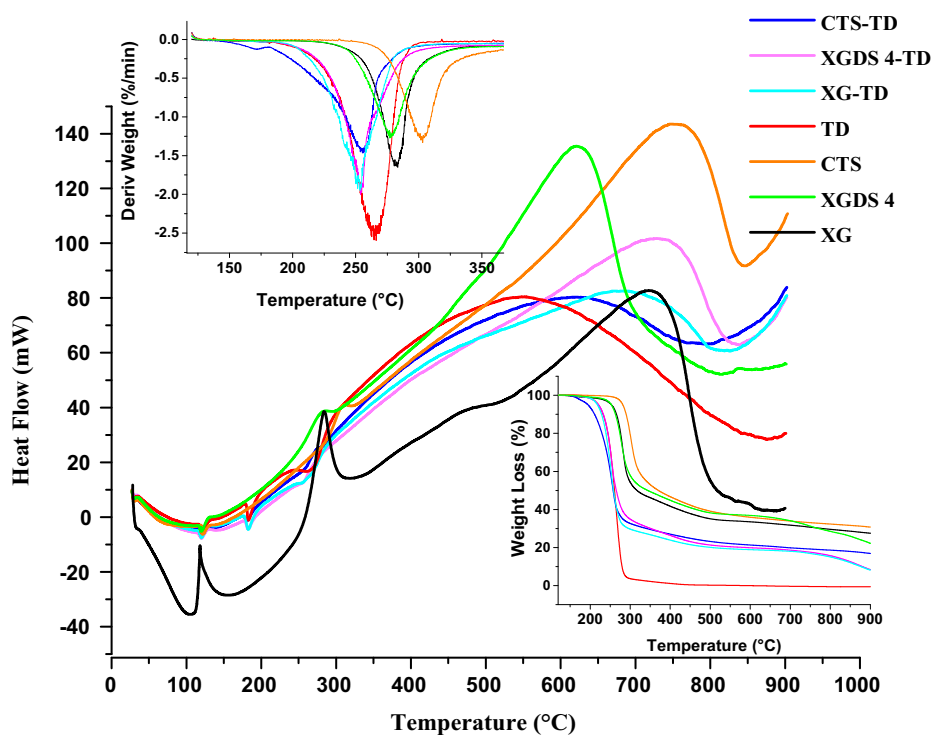


Fig. 7. Thermal study analysis of drug-excipient compatibility: DSC (a), TGA (b) and DTA (c).

not affect the thermal stability of Tramadol (DiNunzio et al.; 2008). Furthermore, it was also shown that none of the tested excipients altered the decomposition profile of the API.

3.3. Characterization of tablets based deacetylated xanthan derivatives and chitosan

3.3.1. Flow properties of powder mixtures

Powder mixtures prepared by using XG, CTS, and XGDSs as matrix excipients showed satisfactory properties (Table 2)

according to the US Pharmacopeia (USP 39, 2016). The values of densities indicate the better die filling and more close packing during the compression of CTS/XGDSs (F2-F5) compared with CTS/XG mixture (F7). These constataions are also confirmed by Carr's index and Hausner's ratio. Indeed, the powder mixtures of CTS/XGDSs (F2-F5) indicated Carr's index values ranged between $9.80 \pm 0.47\%$ and $8.00 \pm 0.54\%$, and Hausner's ratio values from 1.09 ± 0.04 to 1.08 ± 0.02 , reflecting excellent flow properties. On the other hand, XG based formula (F1, F7) and CTS (F6) showed good flow properties with Carr's index values within

Table 2
Flow properties of Tramadol powder mixtures.

Formulation	Static angles of repose*	Bulk density (g/cm ³)*	Tapped density (g/cm ³)*	Carr's index (%)*	Hausner ratio*	Flow Property**
F1	32.53 ± 0.21	0.57 ± 0.02	0.64 ± 0.01	12.28 ± 0.12	1.12 ± 0.01	Good
F2	29.84 ± 0.11	0.51 ± 0.01	0.56 ± 0.04	9.80 ± 0.47	1.09 ± 0.04	Excellent
F3	27.98 ± 0.32	0.52 ± 0.02	0.57 ± 0.02	9.62 ± 0.35	1.10 ± 0.03	Excellent
F4	27.54 ± 0.44	0.53 ± 0.02	0.58 ± 0.02	9.43 ± 0.32	1.09 ± 0.03	Excellent
F5	26.74 ± 0.13	0.50 ± 0.02	0.54 ± 0.02	8.00 ± 0.54	1.08 ± 0.02	Excellent
F6	31.84 ± 0.15	0.53 ± 0.02	0.60 ± 0.02	13.21 ± 0.32	1.13 ± 0.03	Good
F7	32.35 ± 0.24	0.54 ± 0.03	0.61 ± 0.01	12.96 ± 0.46	1.13 ± 0.01	Good

* All values are expressed as mean ± SD, n = 3.

** According to the United States pharmacopeia criteria (USP 39, 2016).

12.28 ± 0.12% to 12.96 ± 0.46%, and Hausner's ratio ranging from 1.12 ± 0.0 to 1.13 ± 0.01. Overall, the obtained results demonstrated that the powder beds of studied formulations (F1-F7) are doted with appreciable flow characteristics and are also easily compressible. Therefore, the use of CTS/XGDSs combinations as tablet excipients, enhanced both compressibility and flowability properties of the powder mixtures.

3.3.2. Physicochemical evaluation of tablets

The variation in diameter, weight, hardness, friability and drug content values of all the prepared tablets were found within standard limits (Table 3). The hardness and friability of all formulations were respectively above 4 kg/cm² and less than 1%, which shows the mechanical stability of the tablets. Therefore, it was noted that both hardness and friability increased with the increasing DD and that desacetylation not only leads to enhanced physical properties of XGDSs but also allows better compressibility and improves the release properties. Drug content was found in the range of 99.92 ± 0.17% to 100.13 ± 0.28%, which meets the USP specifications (USP 39, 2016).

3.3.3. Drug release profiles and dissolution kinetics studies

The main purpose of the formulated tablets is the sustained release of the active ingredient to maintain an effective drug plasma level. In order to investigate the effects of XG, XGDSs and CTS on the kinetics of Tramadol release, the dissolution profiles of set of formulas (F1-F7) were analyzed by plotting the cumulative release data versus time (Fig. 8). During dissolution tests of the matrix tablets, a hydration of their outer layer was noted causing swelling with the formation of an insoluble gelled layer on the extern area of the matrix, following polyelectrolyte complexation between the positively and negatively charged polymers (Ghori et al., 2015; Maderuelo et al., 2011). Over time, hydration progressed from the tablet surface to the center, with slow and gradual erosion of the outer gel layer, exposing a new layer of gel to the dissolution medium. This mechanism was observed for extended-release tablets formed by matrix systems based on polyelectrolyte polysaccharides in several studies (Luo and Wang, 2014; Al-Akayleh et al., 2013; Mughal et al., 2011). Consequently, gel layers formation prevents the initial burst effect and hence retards the

drug release. Indeed, no burst release was observed in any studied formulation (F1-F7), where 10% of TD was released in the range of 0.62 ± 0.04 to 2.02 ± 0.09 h (Fig. 8).

Further analysis showed that 100% of TD was released from all formulated tablets in the time interval of 14–24 h. It is apparent that F1 tablets based on CTS/XG, released 100% of drug after 16 h, while 50% and 90% of TD were released after 5.89 ± 0.12 and 12.91 ± 0.21 h (Fig. 9). Comparing CTS/XG matrix tablets (F1) with F6 and F7 containing only CTS or XG, it can be seen that the tablets prepared with CTS/XG had a significant slower drug release (p < 0.05). These results indicate a synergistic effect resulting from the interpolyelectrolyte complexation between biopolymers leading to the strengthening of matrices based on CTS/XG blends. The obtained results are in agreement with previous works (Kharshoum and Aboutaleb, 2016; Fareez et al., 2015).

For all CTS/XGDSs tablets (F2 to F5), the dissolution rate varied with the DD of XG derivatives, where the higher the DD of XGDS the lower the drug release rates. Among all formulations based on CTS/XGDS blends, formulation F5 (CTS/XGDS4) presented the slowest in-vitro release rate during 24 h, where 50 and 90% of TD was released after 11.19 ± 0.18 h and 20.94 ± 0.21 h (Fig. 9). Furthermore, polymeric mixtures of CTS/XGDSs have increased the overall retardation performance compared with CTS/XG tablets. Although, CTS-XG based tablets obtained by direct compression, showed a considerable potential of drug release retardation, but it is evident that CTS-XGDSs based tablets have increased the sustained release performance of the hydrophilic matrices. This may be due to the large number of hydroxyl groups present on XGDSs chains which induce an instantaneous dipole attraction with the surrounding atoms. Therefore, the hydroxyl groups along the XGDSs chains are more accessible because of the reduced steric hindrance and the lower molecular weight after the desacetylation of XG molecules (Thakur et al., 2014). These factors increase the intermolecular interactions and penetration between branched chains of CTS and XGDSs, producing the formation of more stable CTS-XGDSs complexes. This explains the greater retention capacity of CTS/XGDS4 matrices.

Furthermore, the kinetic study showed that at acidic pH (1.2), the release rate of TD from CTS/XGDS hydrophilic matrices decreased during the first two hours as DD increases, where the

Table 3
Physicochemical evaluation of Tramadol sustained release matrix tablets.

Formulation	Average weight (mg) ^a	Hardness (kg/cm ²) ^b	Friability (%) ^b	Diameter (mm) ^a	Drug content (%) ^b
F1	401.54 ± 2.52	4.85 ± 0.78	0.54 ± 0.02	12.14 ± 0.01	99.98 ± 0.12
F2	401.85 ± 3.25	5.12 ± 0.21	0.62 ± 0.03	12.54 ± 0.02	99.92 ± 0.17
F3	402.14 ± 2.74	5.45 ± 0.14	0.71 ± 0.01	12.41 ± 0.04	100.05 ± 0.25
F4	400.58 ± 2.74	5.69 ± 0.02	0.75 ± 0.02	12.17 ± 0.02	100.07 ± 0.17
F5	401.52 ± 2.54	5.89 ± 0.14	0.78 ± 0.02	12.18 ± 0.02	100.13 ± 0.28
F6	402.14 ± 2.12	4.25 ± 0.08	0.65 ± 0.01	12.32 ± 0.01	99.98 ± 0.16
F7	401.32 ± 3.24	4.56 ± 0.16	0.69 ± 0.02	12.15 ± 0.02	100.12 ± 0.25

All results represent mean ± standard deviation (^an = 20, ^bn = 10).

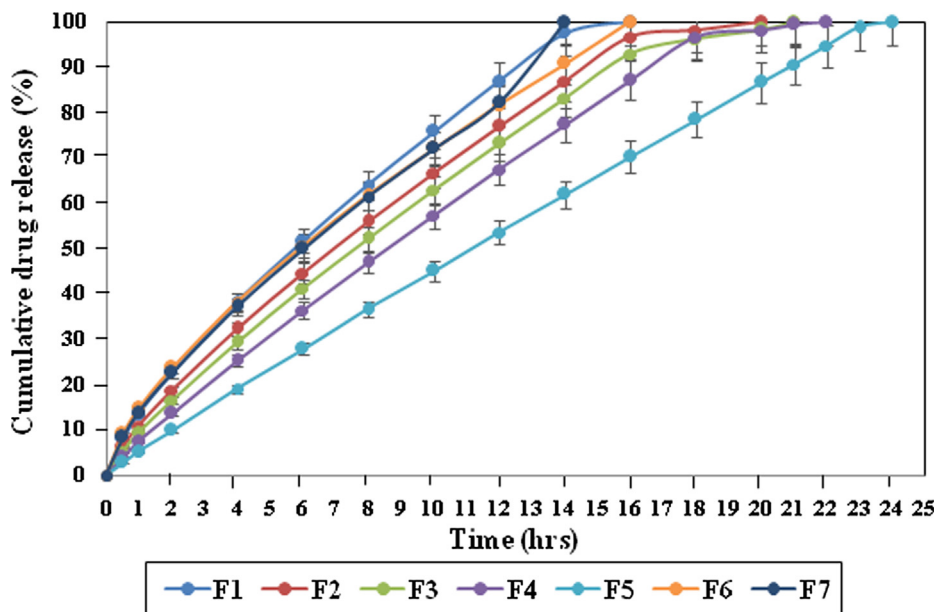


Fig. 8. Drug release profiles of Tramadol matrix tablets (F1-F7).

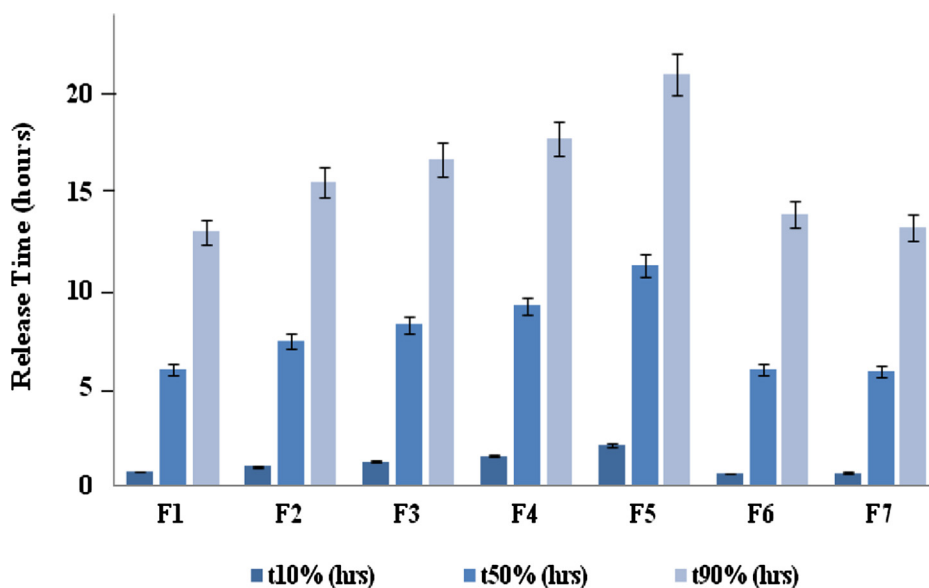


Fig. 9. Effect of formulation composition on the 10%, 50%, and 90% drug release of different formulations.

amounts of TD released vary from 16.56% (F2, XGDS1) to 9.95% (F5, XGDS4). This indicates a higher resistance of XGDSs-based tablets to the acidic medium when the value of DD is higher. While at pH 6.8, a steady and prolonged increase in TD dissolution was observed reaching 24 h for the formula F5. The obtained results demonstrated the influence of DD on the dissolution profiles of TD and also confirmed that the XGDSs derivatives may be considered as interesting excipients in the formulation of sustained release dosage forms.

The release behavior prediction and correlation of TD release from tablets was realized by fitting the dissolution data to Korsmeyer-Peppas mathematical model (Korsmeyer et al., 1983; Siepmann et al., 2002). This model is currently the best way to approach and predict drug release kinetics. It is possible to estimate most of the technological factors such as the optimal

composition, geometry, dimensions and manufacturing methods, necessary to obtain the desired release profiles (Tiwari et al., 2003; Ferrero et al., 2010; Maderuelo et al., 2011). For a thorough understanding of several dissolution mechanisms, it is necessary to interpret the obtained values of the release exponent (n). In the case of tablets, when n is less than 0.45, the drug release is controlled by diffusion, whereas an anomalous transport mechanism is evolved for n values comprised in the range of 0.45–0.89. While, for n values greater than 0.89, the release mechanism of the drug is dominated by the matrix erosion (case II transport) (Siepmann and Peppas, 2001).

The release data of all tested matrix tablets showed that they are well fitted by adequate kinetics models as evidenced by the higher R^2 values (0.996–0.999). The ANOVA-based comparisons were carried out with the percentage of TD released at $t_{10\%}$, $t_{50\%}$

Table 4
Korsmeyer–Peppas semi-empirical model parameters.

Formulation	Korsmeyer–Peppas model			Release time (hours)			Drug release mechanism
	K [% hrs ⁻ⁿ]	N	R ²	t _{10%} (hrs) ^a	t _{50%} (hrs) ^a	t _{90%} (hrs) ^a	
F1	13.218	0.750	0.996	0.69 ± 0.03	5.89 ± 0.12	12.91 ± 0.21	Anomalous transport
F2	10.339	0.790	0.998	0.96 ± 0.05	7.35 ± 0.15	15.47 ± 0.25	Anomalous transport
F3	8.749	0.830	0.998	1.18 ± 0.08	8.17 ± 0.20	16.58 ± 0.19	Anomalous transport
F4	6.985	0.890	0.998	1.50 ± 0.12	9.13 ± 0.05	17.67 ± 0.28	Anomalous transport
F5	5.166	0.940	0.999	2.02 ± 0.09	11.19 ± 0.18	20.94 ± 0.21	Case-II transport
F6	14.725	0.690	0.998	0.57 ± 0.05	5.88 ± 0.21	13.79 ± 0.27	Anomalous transport
F7	14.108	0.720	0.996	0.62 ± 0.04	5.80 ± 0.19	13.114 ± 0.23	Anomalous transport

^a Results represent mean ± standard deviation (n = 6).

and t_{90%} corresponding respectively to the time necessary to release 10%, 50% and 90% of drug. Significant differences between all formulations were found at time points (p < 0.05).

The obtained data confirmed that the TD release mechanism was dominated by matrix swelling and matrix erosion processes (Table 4). The values of *n* were comprised between 0.72 and 0.89 for all formulations, which indicates an anomalous diffusion mechanism coupling diffusion and erosion, except for formulation F5 exhibiting the higher *n* value (0.94) that indicates a Case-II transport mechanism. By the comparison of the exponent *n* values, it was clearly observed that the higher the *n* value, the slower the TD dissolution kinetics. Indeed, in the case of formulation F5, the release times of 10% (2.02 ± 0.09 h), 50% (11.19 ± 0.18 h), and 90% (20.94 ± 0.21 h) of TD indicate that for *n* values close to 1.0, a slower release of drug is observed.

4. Conclusion

The obtained results revealed the utility of use of desacetylated XG combined with chitosan (CTS) as excipients in the pharmaceutical industry. The degree of deacetylation (DD) was found to have an impact on the various properties of desacetylated derivatives (XGDS). The solubility power was found to be substantially decreased with the increase in DD. It was noticed that CTS/XGDS mixtures produced powders with good flow characteristics and tablets with considerable physical properties. Moreover, CTS/XGDS matrices showed a high potential towards sustaining the release of Tramadol. The efficiency of the obtained matrices to retard differently the drug release can be exploited with different DD. The desacetylation of XG imparted its hydrophilicity which significantly prevents the release of drug in dissolution media when associated with CTS. In support of these results, deacetylation reaction led not only to the improvement of the physical properties, but also to those of compressibility and release. Although the oral route is considered the most convenient for administering drugs to patients, the desacetylated derivatives mixed with chitosan can be used for the formulation of other sustained release dosage forms.

Declaration of Competing Interest

The authors declared that there is no conflict of interest.

Acknowledgements

This work was realized as part of a scientific collaboration between the International Iberian Laboratory of Nanotechnology (Portugal) and the Ministry of Higher Education and Scientific Research of Algeria. The authors are also thankful to Sidal Pharmaceutical Company of Medea for the technical support.

References

- Al-Akayleh, F., Al Remawi, M., Rashid, I., Badwan, A., 2013. Formulation and *in vitro* assessment of sustained release terbutaline sulfate tablet made from binary hydrophilic polymer mixtures. *Pharm. Dev. Technol.* 18, 1204–1212.
- Alvarez-Lorenzo, C., Blanco-Fernandez, B., Puga, A.M., Concheiro, A., 2013. Crosslinked ionic polysaccharides for stimuli-sensitive drug delivery. *Adv. Drug Deliv. Rev.* 65, 1148–1171.
- Beakley, B.D., Kaye, A.M., Kaye, A.D., 2015. Tramadol, pharmacology, side effects, and serotonin syndrome: a review. *Pain Phys.* 18, 395–400.
- Bellini, M.Z., Caliarri-Oliveira, C., Mizukami, A., Swiech, K., Covas, D.T., Donadi, E.A., Oliva-Neto, P., Moraes, Á.M., 2015. Combining xanthan and chitosan membranes to multipotent mesenchymal stromal cells as bioactive dressings for dermo-epidermal wounds. *J. Biomater. Appl.* 29, 1155–1166.
- Bhattarai, N., Gunn, J., Zhang, M., 2010. Chitosan-based hydrogels for controlled, localized drug delivery. *Adv. Drug Deliv. Rev.* 62, 83–99.
- Callet, F., Milas, M., Rinaudo, M., 1987. Influence of acetyl and pyruvate contents on rheological properties of xanthan in dilute solution. *Int. J. Biol. Macromol.* 9, 291–293.
- Chen, M.-C., Mi, F.-L., Liao, Z.-X., Hsiao, C.-W., Sonaje, K., Chung, M.-F., Hsu, L.-W., Sung, H.-W., 2013. Recent advances in chitosan-based nanoparticles for oral delivery of macromolecules. *Adv. Drug Deliv. Rev.* 65, 865–879.
- Corti, G., Cirri, M., Maestrelli, F., Mennini, N., Mura, P., 2008. Sustained-release matrix tablets of metformin hydrochloride in combination with triacetyl-β-cyclodextrin. *Eur. J. Pharm. Biopharm.* 68, 303–309.
- DiNunzio, J.C., Miller, D.A., Yang, W., McGinity, J.W., Williams, R.O., 2008. Amorphous compositions using concentration enhancing polymers for improved bioavailability of Itraconazole. *Mol. Pharm.* 5, 968–980.
- Du, X., Li, J., Chen, J., Li, B., 2012. Effect of degree of deacetylation on physicochemical and gelation properties of konjac glucomannan. *Food Res. Int.* 1, 270–278.
- Dumitriu, S., Chornet, E., 1997. Immobilization of xylanase in chitosan-xanthan hydrogels. *Biotechnol. Prog.* 13, 539–545.
- Elsayed, A., Remawi, M.A., Qinna, N., Farouk, A., Badwan, A., 2009. Formulation and characterization of an oily-based system for oral delivery of insulin. *Eur. J. Pharm. Biopharm.* 73, 269–279.
- Fareez, I.M., Lim, S.M., Mishra, R.K., Ramasamy, K., 2015. Chitosan coated alginate-xanthan gum bead enhanced pH and thermotolerance of *Lactobacillus plantarum* LAB12. *Int. J. Biol. Macromol.* 72, 1419–1428.
- Ferrero, C., Massuelle, D., Doelker, E., 2010. Towards elucidation of the drug release mechanism from compressed hydrophilic matrices made of cellulose ethers. II. Evaluation of a possible swelling-controlled drug release mechanism using dimensionless analysis. *J. Control Release* 141, 223–233.
- García-Ochoa, F., Santos, V.E., Casas, J.A., Gómez, E., 2000. Xanthan gum: production, recovery, and properties. *Biotechnol. Adv.* 18, 549–579.
- Ghorai, S., Sarkar, A.K., Panda, A.B., Pal, S., 2013. Effective removal of Congo red dye from aqueous solution using modified xanthan gum/silica hybrid nanocomposite as adsorbent. *Bioresour. Technol.* 144, 485–491.
- Ghori, M.U., Conway, B.R., 2015. Hydrophilic matrices for oral control drug delivery. *Am. J. Pharm. Sci.* 3, 103–109.
- Ghori, M.U., Šupuk, E., Conway, B.R., 2015. Tribo-electrification and powder adhesion studies in the development of polymeric hydrophilic drug matrices. *Materials (Basel)* 8, 1482–1498.
- He, H., Hong, Y., Gu, Z., Liu, G., Cheng, L., Li, Z., 2016. Improved stability and controlled release of CLA with spray-dried microcapsules of OSA-modified starch and xanthan gum. *Carbohydr. Polym.* 147, 243–250.
- Kharshoum, R.M., Aboutaleb, H.A., 2016. Formulation, development and evaluation of meclozine hydrochloride microspheres. *J. Bioeq. Bioav.* 8, 27–32.
- Khouryieh, H., Herald, T., Aramouni, F., Bean, S., Alavi, S., 2007. Influence of deacetylation on the rheological properties of xanthan-guar interactions in dilute aqueous solutions. *J. Food Sci.* 72, C173–C181.
- Korsmeyer, R.W., Gurny, R., Doelker, E., Buri, P., Peppas, N.A., 1983. Mechanisms of solute release from porous hydrophilic polymers. *Int. J. Pharm.* 15, 25–35.
- Kumar, I., Mir, N.A., Rode, C.V., Wakhloo, B.P., 2012. Intramolecular huisgen [3+2] cycloaddition in water: synthesis of fused pyrrolidine-triazoles. *Tetrahedron-Asymmetr.* 23 (3–4), 225–229.

- Li, J., Ye, T., Wu, X., Chen, J., Wang, S., Lin, L., Li, B., 2014. Preparation and characterization of heterogeneous deacetylated konjac glucomannan. *Food Hydrocolloid* 40, 9–15.
- Li, P., Li, T., Zeng, Y., Li, X., Jiang, X., Wang, Y., Xie, T., Zhang, Y., 2016. Biosynthesis of xanthan gum by *Xanthomonas campestris* LREL-1 using kitchen waste as the sole substrate. *Carbohydr. Polym.* 151, 684–691.
- Luo, Y., Wang, Q., 2014. Recent development of chitosan-based polyelectrolyte complexes with natural polysaccharides for drug delivery. *Int. J. Biol. Macromol.* 64, 353–367.
- Mabrouk, M., Beherei, H.H., ElShebiney, S., Tanaka, M., 2018. Newly developed controlled release subcutaneous formulation for tramadol hydrochloride. *Saudi Pharm. J.* 26, 585–592.
- Maderuelo, C., Zarzuelo, A., Lanao, J.M., 2011. Critical factors in the release of drugs from sustained release hydrophilic matrices. *J. Control. Release* 154, 2–19.
- Makhado, E., Pandey, S., Nomngongo, P.N., Ramontja, J., 2018. Preparation and characterization of xanthan gum-cl-poly (acrylic acid)/o-MWCNTs hydrogel nanocomposite as highly effective re-usable adsorbent for removal of methylene blue from aqueous solutions. *J. Colloid Interf. Sci.* 513, 700–714.
- Martínez-Ruvalcaba, A., Chornet, E., Rodrigue, D., 2007. Viscoelastic properties of dispersed chitosan/xanthan hydrogels. *Carbohydr. Polym.* 67, 586–595.
- Martins, A.F., Pereira, A.G., Fajardo, A.R., Rubira, A.F., Muniz, E.C., 2011. Characterization of polyelectrolytes complexes based on N, N, N-trimethyl chitosan/heparin prepared at different pH conditions. *Carbohydr. Polym.* 86, 1266–1272.
- Masuelli, M.A., 2014. Mark-Houwink parameters for aqueous-soluble polymers and biopolymers at various temperatures. *J. Polym. Biopolym. Phys. Chem.* 2, 37–43.
- Mendes, A.C., Baran, E.T., Reis, R.L., Azevedo, H.S., 2013. Fabrication of phospholipid-xanthan microcapsules by combining microfluidics with self-assembly. *Acta Biomater.* 9, 6675–6685.
- Mishra, B., Bakde, B.V., Singh, P.N., Kumar, P., 2006. Development and in-vitro evaluation of oral sustained release formulation of Tramadol hydrochloride. *Acta Pharm. Sci.* 48, 153–166.
- Mughal, M.A., Iqbal, Z., Neau, S.H., 2011. Guar gum, xanthan gum, and HPMC can define release mechanisms and sustain release of propranolol hydrochloride. *AAPS PharmSciTech* 12, 77–87.
- Pergolizzi, J.V., Taylor, R., Raffa, R.B., 2011. Extended-release formulations of tramadol in the treatment of chronic pain. *Exp. Op. Pharmacother.* 12, 1757–1768.
- Popa, N., Novac, O., Profire, L., Lupusoru, C.E., Popa, M.I., 2010. Hydrogels based on chitosan-xanthan for controlled release of theophylline. *J. Mater. Sci. Mater. Med.* 21, 1241–1248.
- Qinna, N., Karwi, Q., Al-Jbour, N., Al-Remawi, M., Alhussainy, T., Al-So'ud, K., Omari, M., Badwan, A., 2015. Influence of molecular weight and degree of deacetylation of low molecular weight chitosan on the bioactivity of oral insulin preparations. *Mar. Drug* 13, 1710–1725.
- Ramasamy, T., Kandhasami, U.D.S., Ruttala, H., Shanmugam, S., 2011. Formulation and evaluation of xanthan gum based aceclofenac tablets for colon targeted drug delivery. *Braz. J. Pharm. Sci.* 47, 299–311.
- Ramasamy, T., Tran, T.H., Cho, H.J., Kim, J.H., Kim, Y.I., Jeon, J.Y., Kim, J.O., 2013. Chitosan-based polyelectrolyte complexes as potential nanoparticulate carriers: physicochemical and biological characterization. *Pharm. Res.* 31, 1302–1314.
- Rekha, M.R., Sharma, C.P., 2009. Synthesis and evaluation of lauryl succinyl chitosan particles towards oral insulin delivery and absorption. *J. Control. Release* 135, 144–151.
- Roy, A., Comesse, S., Grisel, M., Hucher, N., Souguir, Z., Renou, F., 2014. Hydrophobically modified xanthan: an amphiphilic but not associative polymer. *Biomacromolecules* 15, 1160–1170.
- Siddhartha, M., Biswanath, S.A., 2014. Ca-carboxymandhyl xanthan gum mini-matrices: swelling, erosion and their impact on drug release mechanism. *Int. J. Biol. Macromol.* 68, 78–85.
- Siepmann, J., Peppas, N.A., 2001. Modeling of drug release from delivery systems based on hydroxypropyl methylcellulose (HPMC). *Adv. Drug Deliv. Rev.* 48, 139–157.
- Siepmann, J., Streubel, A., Peppas, N.A., 2002. Understanding and predicting drug delivery from hydrophilic matrix tablets using the “sequential layer” model. *Pharm. Res.* 19, 306–314.
- Tako, M., Nakamura, S., 1984. Rheological properties of deacetylated xanthan in aqueous media. *Agri. Biol. Chem.* 48, 2987–2993.
- Thakur, A., Monga, S., Wanchoo, R.K., 2014. Sorption and drug release studies from semi-interpenetrating polymer networks of chitosan and xanthan gum. *Chem. Biochem. Eng. Quart.* 28, 105–115.
- Tinland, B., Rinaudo, M., 1989. Dependence of the stiffness of the xanthan chain on the external salt concentration. *Macromolecules* 22, 1863–1865.
- Tiwari, S.B., Murthy, T.K., Pai, M.R., Mehta, P.R., Chowdary, P.B., 2003. Controlled release formulation of tramadol hydrochloride using hydrophilic and hydrophobic matrix system. *AAPS PharmSciTech.* 4, 18–23.
- USP 39-NF 34 US, 2016. **United States Pharmacopeia and National Formulary, Volumes 1–4. The United States, Pharmacopeial Convention, Inc.: Rockville, MD.**
- Umadevi, S.K., Thiruganesh, R., Suresh, S., Reddy, K.B., 2010. Formulation and evaluation of chitosan microspheres of aceclofenac for colon-targeted drug delivery. *Biopharm. Drug Dispos.* 31, 407–427.
- Vazzana, M., Andreani, T., Fangueiro, J., Faggio, C., Silva, C., Santini, A., Garcia, M.L., Silva, A.M., Souto, E.B., 2015. Tramadol hydrochloride: pharmacokinetics, pharmacodynamics, adverse side effects, co-administration of drugs and new drug delivery systems. *Biomed. Pharmacother.* 70, 234–238.
- Veiga, I.G., Moraes, Â.M., 2012. Study of the swelling and stability properties of chitosan-xanthan membranes. *J. Appl. Polym. Sci.* 124, E154–E160.
- Volod'ko, A.V., Davydova, V.N., Chusovitin, E., Sorokina, I.V., Dolgikh, M.P., Tolstikova, T.G., Balagan, S.A., Galkin, N.G., Yermak, I.M., 2014. Soluble chitosan-carrageenan polyelectrolyte complexes and their gastroprotective activity. *Carbohydr. Polym.* 101, 1087–1093.
- Wen, H., Park, K., 2011. *Oral Controlled Release Formulation Design and Drug Delivery: Theory to Practice.* John Wiley & Sons Inc, Hoboken, New Jersey.
- Wise, D.L., 2000. *Handbook of Pharmaceutical Controlled Release Technology.* Taylor & Francis.
- Yahoum, M.M., Moulai-Mostefa, N., Le Cerf, D., 2016. Synthesis, physicochemical, structural and rheological characterizations of carboxymethyl xanthan derivatives. *Carbohydr. Polym.* 154, 267–275.
- Yihong, Q., 2009. Development of modified release oral solid dosage forms. In: Yihong, Q., Yisheng, C., Zhang, G.Z. (Eds.), *Developing Solid Oral Dosage Forms: Pharmaceutical Theory and Practice.* Elsevier.
- Zohuriaan, M.J., Shokrolahi, F., 2004. Thermal studies on natural and modified gums. *Polym. Test.* 23, 575–579.